IOP Conf. Series: Materials Science and Engineering **266** (2017) 012013 doi:10.1088/1757-899X/266/1/012013

Design of welding parameters for laser welding of thin-walled stainless steel tubes using numerical simulation

M Nagy and M Behúlová

Slovak University of Technology in Bratislava, Faculty of Materials Science and Technology in Trnava, Ulica Jána Bottu č. 2781/25, 917 24 Trnava, Slovakia

mate.nagy@stuba.sk

Abstract. Nowadays, the laser technology is used in a wide spectrum of applications, especially in engineering, electronics, medicine, automotive, aeronautic or military industries. In the field of mechanical engineering, the laser technology reaches the biggest increase in the automotive industry, mainly due to the introduction of automation utilizing 5-axial movements. Modelling and numerical simulation of laser welding processes has been exploited with many advantages for the investigation of physical principles and complex phenomena connected with this joining technology. The paper is focused on the application of numerical simulation to the design of welding parameters for the circumferential laser welding of thin-walled exhaust pipes from theAISI 304 steel for automotive industry. Using the developed and experimentally verified simulation model for laser welding of tubes, the influence of welding parameters including the laser velocity from 30 mm.s^{-1} to 60 mm.s^{-1} and the laser power from 500 W to 1200 W on the temperature fields and dimensions of fusion zone was investigated using the program code ANSYS. Based on obtained results, the welding schedule for the laser beam welding of thin-walled tubes from the AISI 304 steel was suggested.

1. Introduction

The laser beam welding represents a very powerful, productive and efficient technology of joining of various materials, which is used in many industries, from the automotive, aviation, space industries through electronics, medicine to energetic or military industries [1-10]. Modelling and numerical simulation of laser welding processes has been exploited with many advantages for the investigation of physical principles and complex phenomena connected with this joining technology [11-16]. It is generally considered as an effective tool for definition of appropriate welding parameters and optimization of laser welding processes [3, 17-18].

Initial experiments in the field of welding of thin-walled tubes from the AISI 304 stainless steel by solid-state lasers have been carried out in 1974 mainly for the needs of the energy industry in the Europe and America. Up to the present, a large number of reactors and heat exchangers for European nuclear power plants are made from the AISI 304 steel. This steel is also widely used in the automotive industry around the world [5, 19-20].

The main objective of this paper is to design proper welding parameters for the production of weld joints of thin-walled exhaust system tubes from the AISI 304 steel using the solid-state disk laser. To predict the temperature fields in welded pipes, numerical simulation of the laser beam welding in the program code ANSYS is exploited.

2. Problem description

The tubes with the inner diameter of 27.1 mm, the thickness of 0.8 mm and the length of 200 mm from the AISI 304 stainless steel with the chemical composition given in the Table 1 should be welded using the solid-state disk laser TRUMPF TruDisk 4002 with the wavelength of 1063 nm, the fiber diameter of 200 μm and the maximum power of 2 kW [21]. Argon gas with the maximum flow rate of 30 $l.min^{-1}$ can be used as a shielding gas to protect both, weld bead and weld root. To design the appropriate laser power for required welding speed from 30 $mm.s^{-1}$ to 60 $mm.s^{-1}$, numerical simulation of the laser welding was performed using the program code ANSYS [22].

Table 1. Chemical composition of the AISI 304 steel.

Element	C	Cr	Ni	Mn	Si	P	S	Fe
wt. [%]	max. 0.08	18 - 20	8 - 10.5	max. 2.0	max. 1.0	0.045	0.03	bal.

3. Simulation model

In general, numerical modelling is understood as a set of research activities associated with the development of appropriate geometrical model for an investigated object, setting its material properties, definition of relations between the modelled object and surroundings and also verification and validation of created simulation model for the analysed process or system. Hence, the simulation model consists of several parts including geometrical, finite element and material model. An important part constitutes the assignment of loads and boundary conditions. In case or transient processes, the definition of initial conditions is also required.

Numerical simulation of laser beam welding processes requires to solve a coupled thermal, fluid and stress-strain problem involving phase transformations [11, 23-25]. Transient temperature fields developed during the fusion welding can be described by the heat diffusion partial differential equation in the form [26]

$$\rho c_{\mathrm{p}} \frac{\partial T}{\partial t} = \left[\frac{\partial T}{\partial x}\left(\lambda_{\mathrm{x}} \frac{\partial T}{\partial x} \right) + \frac{\partial T}{\partial y}\left(\lambda_{\mathrm{y}} \frac{\partial T}{\partial y} \right) + \frac{\partial T}{\partial z}\left(\lambda_{\mathrm{z}} \frac{\partial T}{\partial z} \right) \right] + q_v . \tag{1}$$

where T is the temperature [°C], t is the time [s], ρ is the density [$kg.m^{-3}$], c_p is the specific heat [$J.kg^{-1}.K^{-1}$], λ is the thermal conductivity [$W.m^{-1}.K^{-1}$] in the x, y, z directions of Cartesian coordinate system and q_v represents the heat generated in the unit volume of material per unit time [$W.m^{-3}$], i. e. the volumetric density of internal heat sources due to the welding heat input. To solve the Fourier-Kirchhoff partial differential equation (1), it is necessary to specify geometrical shapes and dimensions of welded components, thermo-physical properties of welded materials, initial temperature distribution at the beginning of a welding process, intensity of internal heat sources and the thermal effects at the interface of welded structures and environment.

According to the symmetry of investigated welding process and the main aim of numerical simulation (setting of welding parameters), only a one half of a welded tube with the length of 20 mm was taken into account. The designed geometrical model is illustrated in Figure 1a.

To perform the transient thermal analysis, 3D finite element mesh (Figures 1b and 1c) was generated according to supposed temperature gradients using the eight-node 3D element type of SOLID 70 [22]. That means that progressive meshing with the higher elements density in the region of the weld pool and in the heat affected zone (HAZ) was used. The length of elements along the welding line was 0.2 mm. Through the tube thickness, twelve elements were generated for the accurate modelling of the volumetric heat source (Figure 1d) and thus, attaining reasonable temperature distribution in the region of a weld joint. The overall number of elements and nodes was 66 647 and 65 022, respectively.

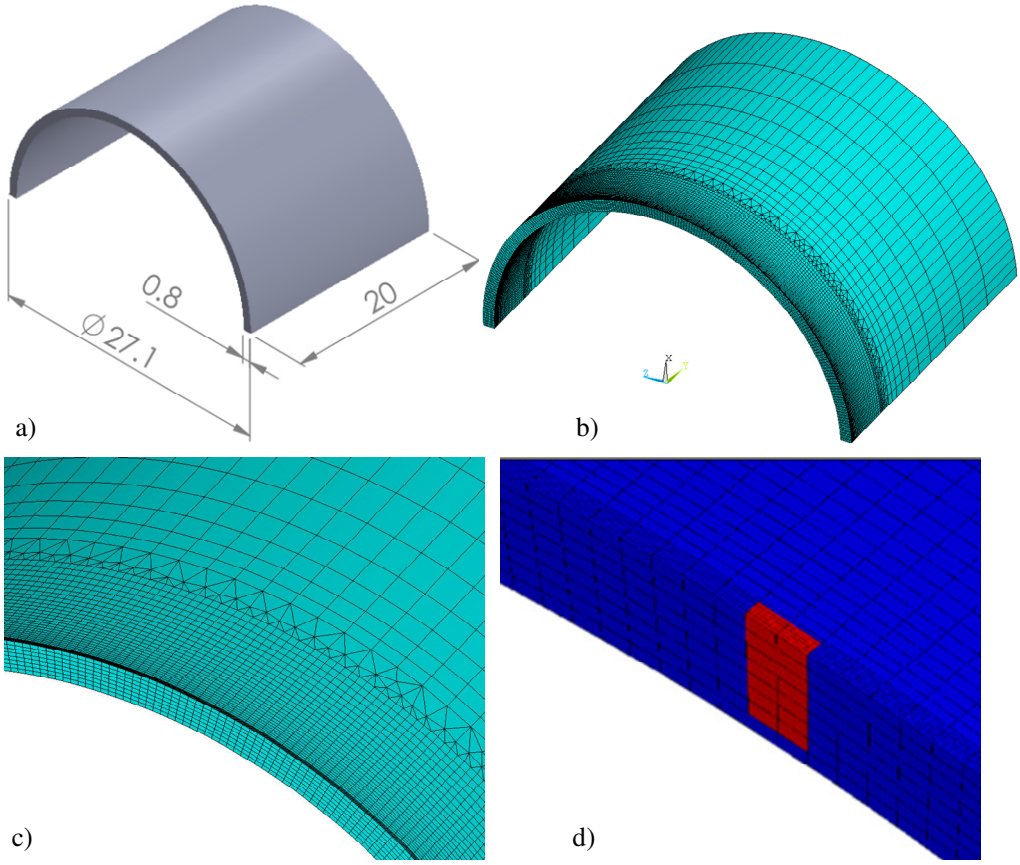

Figure 1. Geometrical model (a) and FE model (b) with a detail of generated mesh (c) and applied volumetric heat source (d).

The thermal properties of the AISI 304 steel in the dependence on temperature (Figure 2) were computed using the JMatPro software [27]. The equilibrium solidus and liquidus temperatures for this steel were computed to be 1360 °C and 1440 °C, respectively. The enthalpy of fusion was modelled applying the method of modified specific heat [28-29].

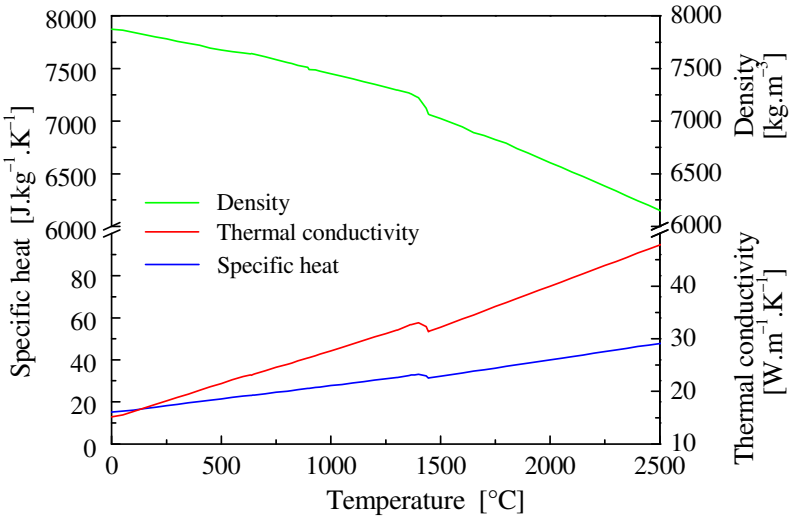

Figure 2. Thermal properties of the AISI 304 steel in the dependence on temperature.

Considering the small thickness of welded tubes and the low thermal conductivity of AISI 304 steel, a simple volumetric heat source model was applied for simulation of laser beam welding. The volumetric density of internal heat sources q_v [W.m^{-3}] was computed by the relationship

$$q_v = \frac{\eta P}{V} \tag{2}$$

where P is the laser power [W], V represents the volume of a heat source [m^3] and η is the efficiency. Depending on the applied laser (mainly the laser wavelength and power), welded material, its phase state, surface quality, temperature and other parameters, the laser energy irradiating the surface of welded material can be partially absorbed, reflected and transmitted. The process efficiency is mainly affected by absorption of laser energy. Based on the literature data, the absorption coefficient for the AISI 304 stainless steel was established to be 37.4 % [30].

The initial temperature of welded tubes was supposed to be 20 °C. The cooling of welded components by convection and radiation to the ambient air and the argon shielding gas was neglected in this case as the heat extraction from the weld bead to the surrounding tube base material by conduction is significantly more important.

4. Verification of simulation model by experimental laser welding

Experimental laser beam welding of thin-walled tubes from AISI 304 stainless steel with the inner diameter of 25.5 mm, the thickness of 0.8 mm and the length of 200 mm was carried out using a solid state DY044 Nd:YAG diode laser from ROFIN-SINAR Laser GmbH company as the disk laser TRUMPF TruDisk 4002 was not available for experimental measurements. The basic technical parameters of the DY044 Nd:YAG diode laser are summarized in Table 2.

Table 2. Technical parameters of a solid state DY044 Nd:YAG diode laser.

Parameter	Value	Units
Maximum power	4.4	kW
Wave length	1053	μm
Beam quality	12	mm.mrad
Laser beam diameter	400	μm

The welded tubes were clamped into a rotary chuck. The welding speed was limited by the maximal speed of applied dog rotary chulk which was 17 mm.s^{-1}. To investigate the influence of welding speed on the quality of produced weld joints, the welding speeds of 10 mm.s^{-1}, 14 mm.s^{-1} and 17 mm.s^{-1} were used. The laser power was varied from 400 W to 1000 W. During experimental laser beam welding, the temperatures were measured by two thermocouples of the K type. The thermocouples were welded by hand on the both sides of weld joints. In this reason, the location of thermocouples was not the same for all samples. The distance of thermocouples from the weld centerline were *a* (thermocouple TC1) and *b* (thermocouple TC2) according to Figure 3a. The welding parameters exploited for the preparation of experimental weld joints are given in Table 3.

Experimentally measured temperatures in the dependence on time for the laser power of 600 W, 800 W and 1000 W are plotted in Figures 3b-d. As it follows from these figures, the maximum measured temperatures are influenced not only by the laser power and welding speed but also very significantly by the distance of thermocouples from the welding centerline. The maximum temperatures on the level of 602 °C and 735 °C were recorded for the laser power of 600 W and the welding speed of 10 mm.s^{-1} and the laser power of 1000 W and the welding speed of 14 mm.s^{-1}, respectively, with the thermocouples located the closest to the centre of the weld joint. Due to the more distant location of thermocouples during the laser welding with higher welding speeds and the same laser power of 800 W, the temperatures measured during the welding with the welding speed of

10 mm.s^{-1} are lower than that measured by the welding with the welding speed of 17 mm.s^{-1} and also 14 mm.s^{-1} (Figure 3c).

Table 3. Welding parameters and position of thermocouples in performed experiments.

Sample	*w* [mm.s^{-1}]	*P* [W]	Distance of thermocouples TC1 and TC2 from the welding line	
			a [mm]	*b* [mm]
1	10	400	6.85	6.36
2	10	600	1.30	2.11
3	10	800	6.83	6.27
4	14	600	2.53	3.75
5	14	800	3.48	4.33
6	14	1000	1.46	1.36
7	17	600	3.72	3.56
8	17	800	2.31	2.61
9	17	1000	6.17	6.48

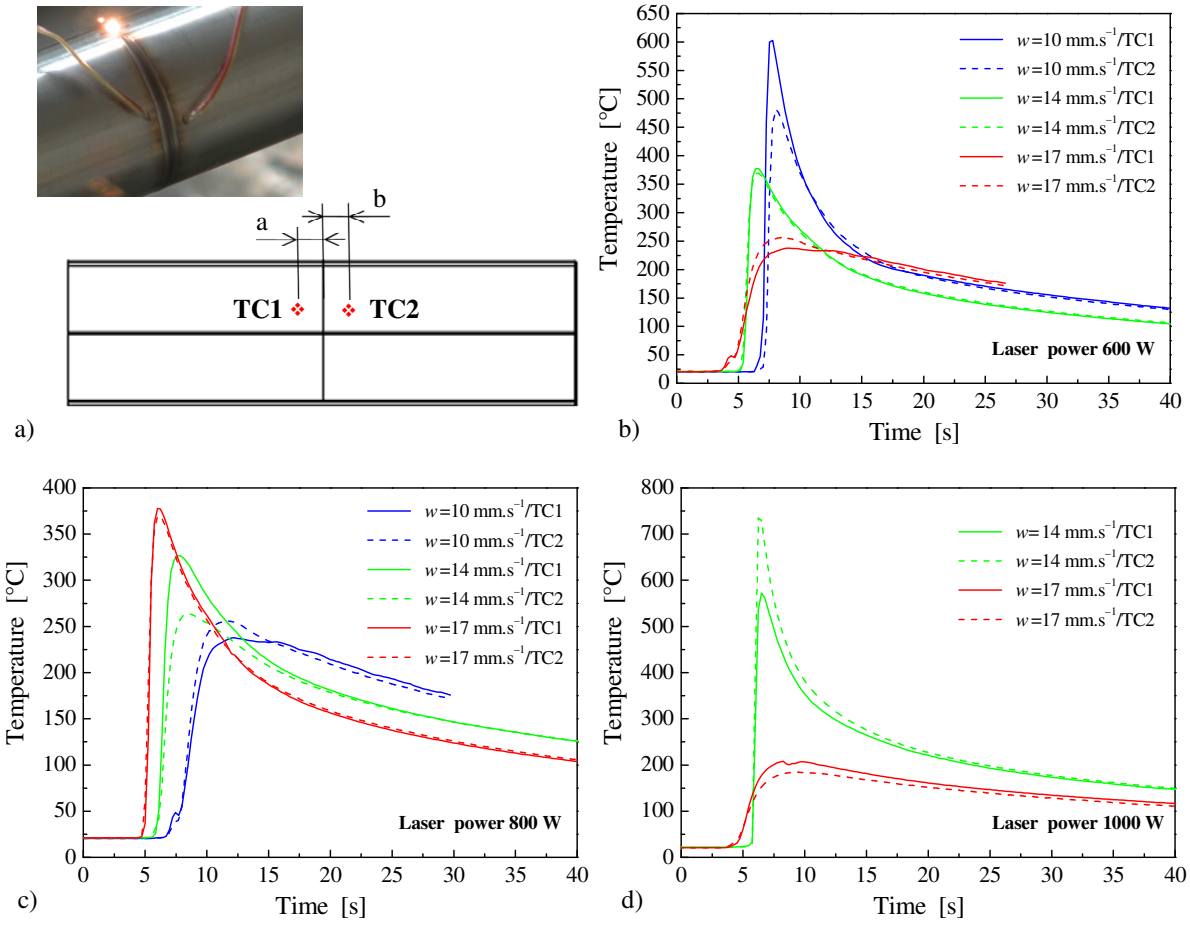

Figure 3. Schematic illustration of the thermocouple positioning (a) and the time dependence of measured temperatures with the laser power of a) 600 W, b) 800 W and c) 1000 W using different welding speeds.

In Figure 4, the measured and computed time histories of temperatures during the laser welding with chosen parameters are compared together with the appearance of produced weld joints. The computed temperatures correspond to the results obtained in the node located at the distance „*a*" indicating in the graphs, i. e. in the node nearest to the position of the thermocouple TC1 or TC2. For the laser power of 600 W and the velocities of 10 mm.s^{-1} and 17 mm.s^{-1} (Figure 4a, c), the distance of corresponding nodes from the weld centerline is smaller than the distance of thermocouple what results in higher maximal computed temperatures in comparison with the measurements. On the other hand, in the case illustrated in Figure 4b (P = 1000 W and w = 17 mm.s^{-1}), the thermocouple TC1 is located closer to the centre of the weld joint than the corresponding node, so the maximum temperature measured by the thermocouple TC1 is higher.

In all investigated cases, the computed temperature decrease during the weld cooling is not as rapid as during the measurements. In simulation model, the weld cooling to the shielding gas and to the environment was neglected and in this reason the computed temperatures during the cooling phase are slightly higher. However, based on the comparison of measured and calculated temperatures it can be concluded that the simulation model was prepared correctly and it can be used for the following computation in order to set proper welding parameters for the laser welding of thin-walled tubes from the AISI 304 stainless steel.

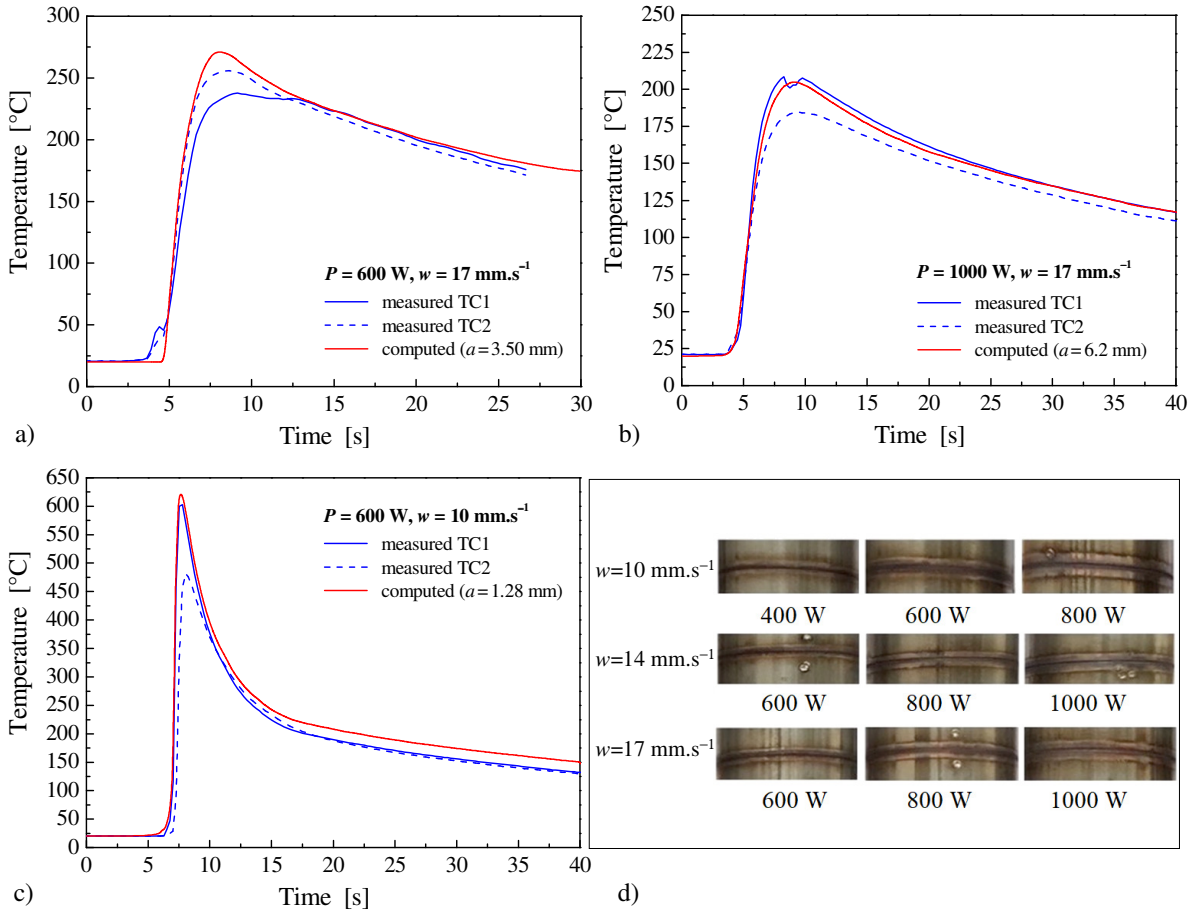

Figure 4. Comparison of measured and computed time histories of temperatures during the laser welding with chosen parameters and the appearance of produced weld joints.

5. Results and discussion

The developed and verified simulation model was applied for the design of welding parameters for the laser welding of the thin-walled tubes from the AISI 304 steel. A set of numerical simulations in the program code ANSYS was carried out with the welding speed varied from the required interval from 30 mm.s^{-1} to 60 mm.s^{-1} and the supposed values of laser power from 500 W to 1200 W.

For illustration, the temperature fields computed applying chosen welding parameters are depicted in Figure 5. The increase in the laser power at the constant welding speed results in the enlargement of a fusion zone and as well as in the enhancement of the maximum temperature of the weld metal (Figure 5a-c). On the other hand, with the increase in welding speed, the size of a fusion zone decreases (Figure 5d-f). The highest temperatures in fusion zone were reached when the combination of high laser power and low welding speed was applied.

In Figure 6, the temperatures of a weld pool and a weld root are shown for considered welding speeds and chosen values of laser power. Based on presented time-temperature dependences, the maximum temperatures attained at the top of the weld pool can be estimated and the possibility of the weld root re-melting can be assessed.

For the welding speed of 30 mm.s^{-1} and the laser power of 500 W, the maximum temperature of the weld root is deeply below the liquidus and also the solidus temperature of the AISI 304 steel. This laser power is insufficient for the production of a sound weld joint. By the laser power of 700 W, the weld root can be re-melted as the maximum weld root temperature reaches the liquidus temperature T_L. In case of welding with the higher laser power (800 W and more), the weld root temperatures are too high.

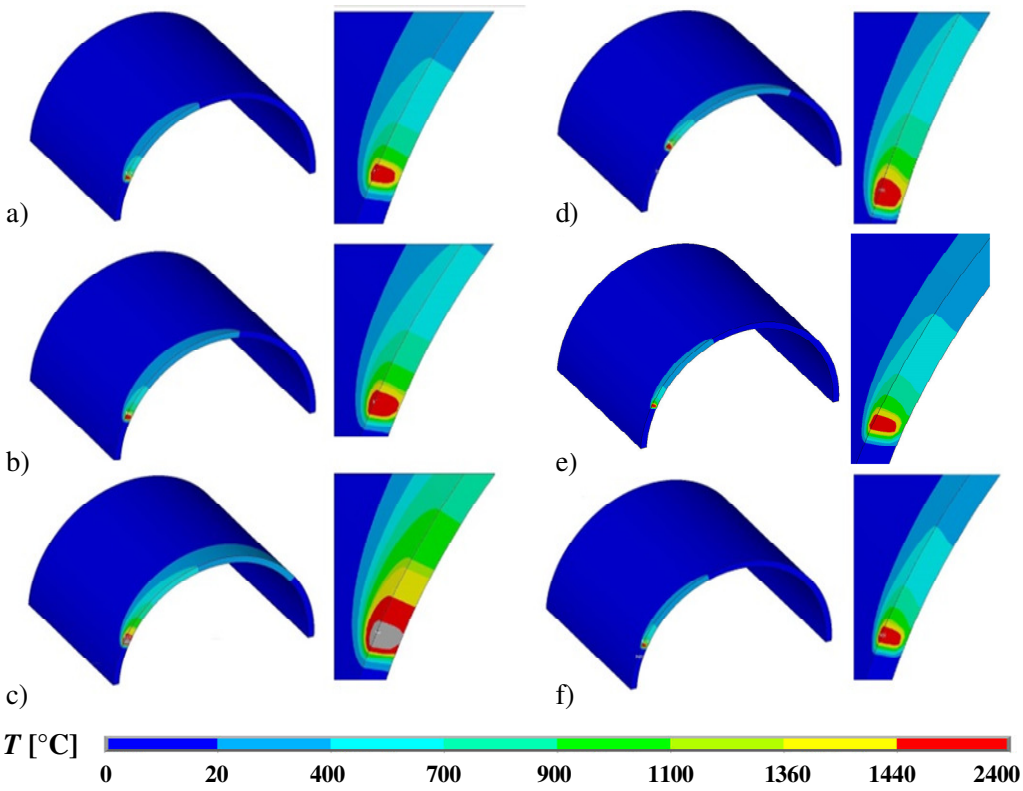

Figure 5. Temperature distribution in a welded tube during the laser welding with the chosen welding parameters: welding speed of 17 mm.s^{-1} and the laser power of a) 500 W, b) 600 W, c) 1000 W and d) the welding speed of 30 mm.s^{-1} and the laser power of 800 W, e) the welding speed of 50 mm.s^{-1} and the laser power of 800 W, f) the welding speed of 60 mm.s^{-1} and the laser power of 900 W.

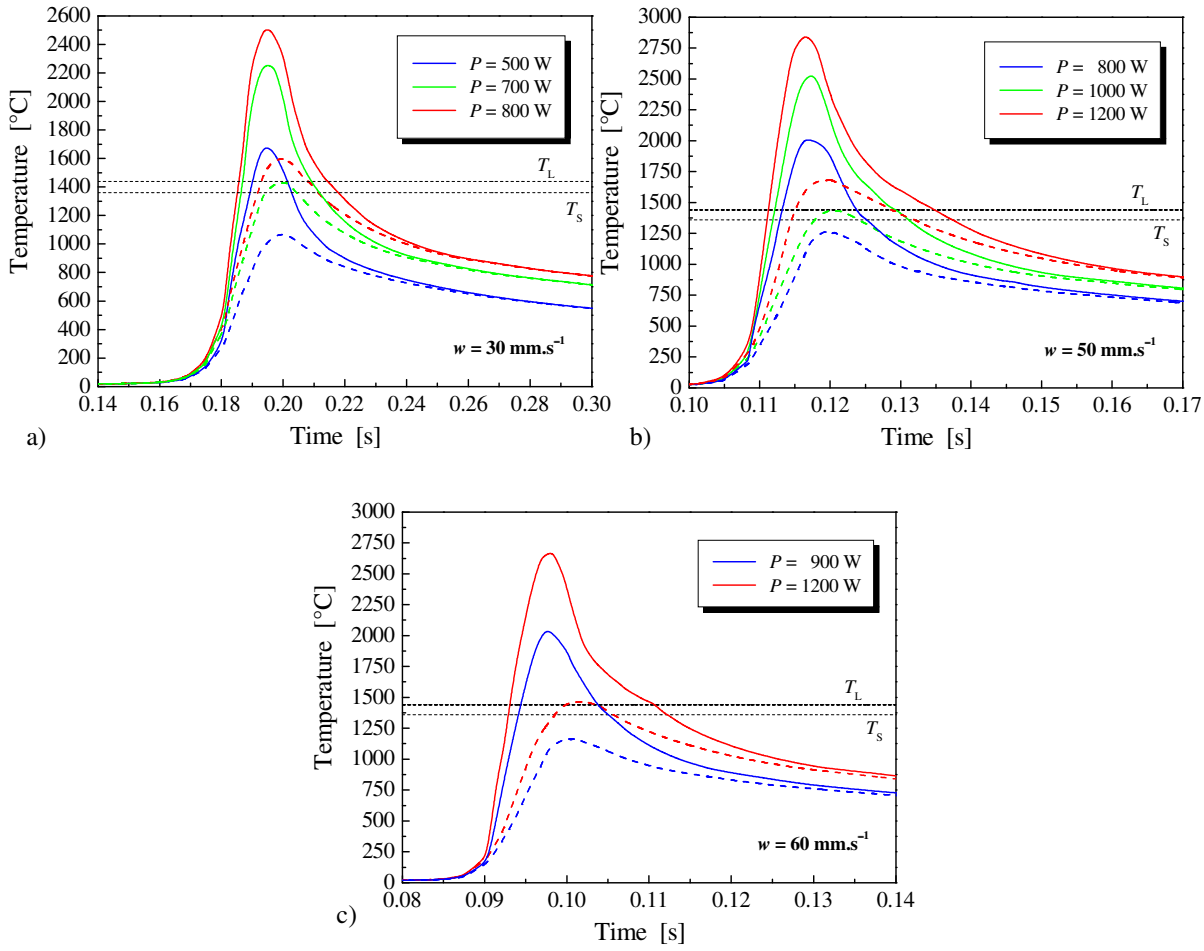

Figure 6. Time dependence of the temperatures at the top of weld pool and on the weld root computed for the welding speed of a) 30 mm.s^{-1}, b) 50 mm.s^{-1} and c) 60 mm.s^{-1} and the chosen values of laser power.

Similarly, the laser power of 800 W and 900 W is not sufficient for the production of high-quality weld joint of tubes from AISI 304 steel if the welding speed is 50 mm.s^{-1} or more. The temperatures of a weld pool using the laser power of 1200 W together with the welding speed of 50 mm.s^{-1} are very high. They can lead to the unwanted boiling of the weld metal.

Based on performed numerical simulations, the welding schedule for laser beam welding of thin-walled tubes from the AISI 304 steel was proposed for the required welding speeds from 30 mm.s^{-1} to 60 mm.s^{-1} (Figure 7). In this figure, the details of temperature distribution in the longitudinal weld cross-section for considered welding parameters are shown. In the grey-coloured regions, the temperatures are above the 2100 °C.

Figure 7 clearly indicates in which cases the tube wall is re-melted through the whole thickness and which welding parameters can be appropriate for the production of high-quality weld joints. For the welding speed of 30 mm.s^{-1}, the minimal laser power must be 700 W. The application of laser powers above 800 W can cause boiling and evaporation of the weld metal. For the welding speed of 50 mm.s^{-1}, the laser power from the interval from 900 W to 1000 W can be recommended. For the highest considered welding speed of 60 mm.s^{-1}, the minimal laser power of 1000 W is required. However, the laser power more than 1100 W can lead to the weld pool temperature increase above the boiling temperature of the AISI 304 steel.

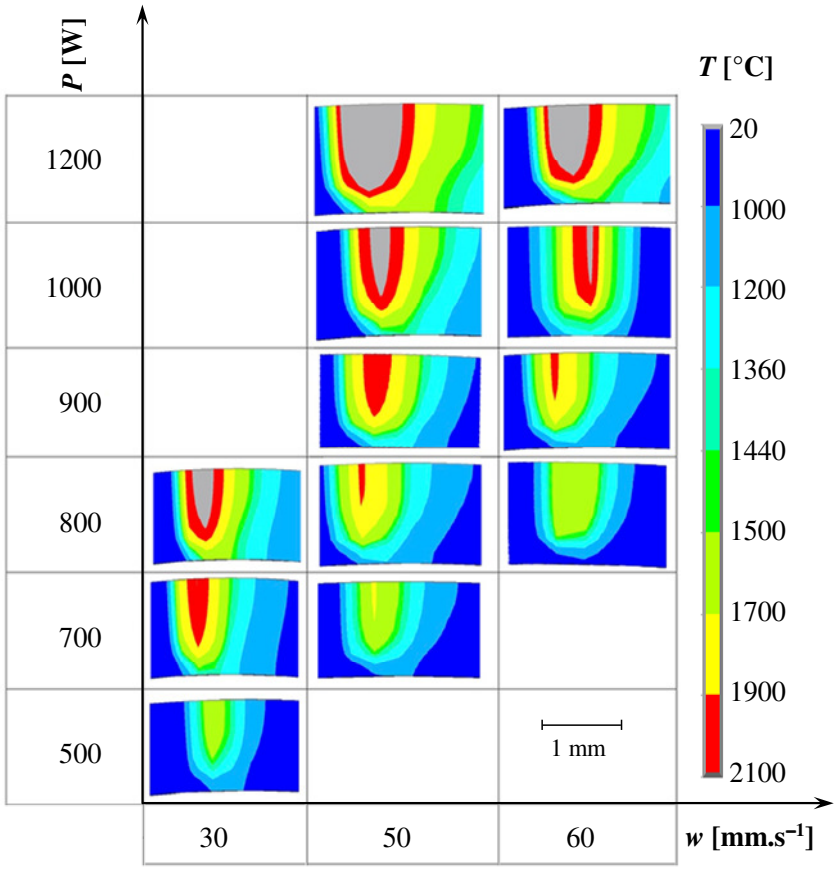

Figure 7. Welding schedule for the laser beam welding of thin-walled tubes from the AISI 304 steel.

6. Conclusions

Based on the developed and verified simulation model, the temperature fields during the process of laser beam welding of thin-walled tubes from the AISI 304 steel were investigated and analysed. According to obtained results, the following values of laser power can be recommended for the production of sound weld joints of thin-walled tubes from AISI 304 stainless steel using the solid-state disc laser TRUMPF TruDisk 4002 and required welding speeds:

- the laser power from 700 W to 800 W for the welding speed of 30 mm.s^{-1},
- the laser power from 900 W to 1100 W for the welding speed of 50 mm.s^{-1} and
- the laser power from 1000 W to 1200 W for the welding speed of 60 mm.s^{-1}.

Acknowledgments

The research has been supported by the Scientific Grant Agency of the Slovak Republic (VEGA) within the project No. 1/1010/16 and the Programs to support excellent young researchers and research teams (NUM-LBW-FE/Al and 1347/PRO-MAT-ZVAR) of the STU Bratislava.

References

[1] Katayama S 2013 *Handbook of Laser Welding Technologies*. A volume in Woodhead Publishing Series in Electronic and Optical Materials (Cambridge: Woodhead Publishing Limited)

[2] Lawrence J 2008 *Advances in Laser Materials Processing, Technology, Research and Application.* A volume in Woodhead Publishing Series in Welding and Other Joining Technologies (Cambridge: Woodhead Publishing Limited)

[3] Michalos G et al. 2010 Automotive assembly technologies review: challenges and outlook for a flexible and adaptive approach *CIRP-JMST* **2** 81-91
[4] Rossini M et al. 2015 Investigation on dissimilar laser welding of advanced high strength steel sheets for the automotive industry *Mat Sci Eng A-Struct* **628** 288-296
[5] Hong K Yand Shin C 2017 Prospects of laser welding technology in the automotive industry: A review *J Mater Process Tech* **245** 46-69
[6] Choudhury B and Chandrasekaran M 2017 Investigation on welding characteristics of aerospace materials – A review *Materials Today*: *Proceedings* **4** 8 7519-7526
[7] Blackburn J 2012 *Laser welding of metals for aerospace and other applications* A volume in Woodhead Publishing Series in Welding and Other Joining Technologies (Cambridge: Woodhead Publishing Limited) pp 75–108
[8] Reitemeyer D, Schultz V, Syassen F, Seefeld T and Vollertsen F 2013 Laser Welding of Large Scale Stainless Steel Aircraft Structures *Physics Proc* **41** 106-111
[9] Moraitis G A and Labeas G N 2009 Prediction of residual stresses and distortions due to laser beam welding of butt joints in pressure vessels *Int J Pres Ves Pip* **86** 2–3 133-142
[10] Zhou Y N and Breyen Mark D 2013 *Joining and Assembly of Medical Materials and Devices.* A volume in Woodhead Publishing Series in Biomaterials (Cambridge: Woodhead Publishing Limited)
[11] Dal M and Fabbro R 2016 An overview of the state of art in laser welding simulation *Opt Laser Technol* A **78** 2-14
[12] Chukkan R J et al 2015 Simulation of laser butt welding of AISI 316L stainless steel sheet using various heat sources and experimental validation *J Mat Process Techn* **219** 48-59
[13] Mackwood P and Craferb R C 2004 Thermal modelling of laser welding and related processes: a literature review *Opt Laser Technol* **37** 99
[14] Frewin M R and Scott D A 1999 Finite Element Model of Pulsed Laser Welding *Weld J* **78** 5-22
[15] Lindgren L E 2004 Numerical modelling of welding *Comput Methods Appl Mech Eng* **195** 48-49 6710-6736
[16] Olabi A G and Gasalino G 2014 Mathematical modeling of weld phenomena part I Finite element modeling *Reference Module in Materials Science and Materials Engineering, Comprehensive Materials Processing* **6** 101-109
[17] Nagel F, Simon F, Kümmel B, Bergmann J P and Hildebrand J 2014 Optimization Strategies for Laser Welding High Alloy Steel Sheets *Physics Proc* **56** 1242-1251
[18] Sokolov M, Salminen A, Khlusova E I, Pronin M M, Golubeva M and Kuznetsov M 2015 Testing of New Materials and Computer Aided Optimization of Laser Beam Welding of High-Strength Steels *Physics Proc* **78** 255-264
[19] Ashby M F and Smidman M 2010 *Materials for Nuclear Power Systems* (Granta material inspiration) 1-20
[20] Xu J et al 2017 Comparison of residual stress induced by TIG and LBW in girth weld of AISI 304 stainless steel pipes *J Mat Process Techn* **248** 178-184
[21] https://www.trumpf.com/en_GB/products/laser/disk-lasers/trudisk/
[22] ANSYS Inc. Computer software Pennsylvania, United States
[23] Lindgren L E 2001 Finite element modelling and simulation of welding *J Ther Stresses* **24** 141-192
[24] Souloumiac B, Boitout F and Bergheau J-M 2002 A new local global approach for the modelling of welded steel component distortions, *Math Modelling Ser **6*** 573–590
[25] Deng D 2009 FEM prediction of welding residual stress and distortion in carbon steel considering phase transformation effects *Mater Design* **30** 2 359-366
[26] Incropera P F and De Witt D P 1996 *Fundamentals of heat and mass transfer* (New York: J. Wiley and Sons)
[27] JMatPro Help, Release 6.1 2012 Sente Software Ltd
[28] Huy H and Argyropoulos S A 1996 Mathematical modelling of solidification and melting: a review *Model Simul Mater Sc* **4** 371–396

[29] Yau Ch L Chao L S 2006 Modified Effective Specific Heat Method of Solidification Problems *Mater Trans* **47** 2737-2744
[30] Bergström D 2008 *The Absorption of Laser Light by Rough Metal Surfaces* - Doctoral Thesis (Luleå: Luleå University of Technology, Sweden)